2024 IEEE 63rd Conference on Decision and Control (CDC)
December 16-19, 2024. MiCo, Milan, Italy

Output-feedback-based affine formation manoeuvre control of multi-agent systems applying negative imaginary systems theory

Yu-Hsiang Su, Parijat Bhowmick, *Member, IEEE*, and Alexander Lanzon, *Senior Member, IEEE*

***Abstract*— This paper exploits the Negative Imaginary systems theory to develop a novel affine formation manoeuvre control framework for multi-agent systems using dynamic output feedback. The framework begins by deriving affine transformation matrices for leader agents, enabling dynamic adjustments from the nominal formation to the target formation. An output-feedback distributed Strictly Negative Imaginary control law is then proposed for follower agents to achieve affine formation manoeuvres. Unlike existing affine formation manoeuvre control schemes, which typically rely on full-state feedback (including both position and velocity measurements), the proposed approach requires only relative position measurements. In addition, it offers more freedom in choosing a dynamic controller transfer function, thereby improving formation tracking performance. A comprehensive simulation case study is provided to test the effectiveness of the proposed output-feedback-based affine formation manoeuvre control framework.**

I. Introduction

Formation control of multi-agent systems (MASs) has been a major focus of research within the control community over the past two decades. It is generally divided into two main sub-problems: (a) formation shape control and (b) formation manoeuvre control [1]. Formation shape control involves steering networked agents to maintain a specific geometric shape. In contrast, formation manoeuvre control is more complex, as it requires not only maintaining the geometric shape but also enabling transitional, rotational, scaling, shearing, and combined movements [2], as illustrated in Fig. 1. These manoeuvres have practical applications in many real-world scenarios, such as search and navigation missions, where networked agents must adapt their speed, direction, orientation and the size of the entire formation shape to navigate through obstacles and corridors in cluttered environments [3]–[5]. Existing formation controllers that use graph Laplacian matrices are typically categorised into three types based on how formation constraints are specified, such as displacement-based [4]–[6], distance-based [7] and bearing-based [8]. However, these approaches have limitations in tracking formation translational, rotational, scaling, and shearing movements, as they often require changes to the formation constraints [1] or additional observer designs [9] to handle these movements effectively.

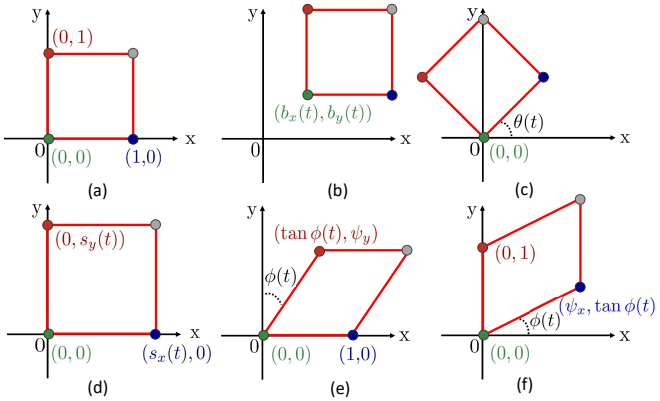

Fig. 1. Affine formation manoeuvres in a two-dimensional space. (a) The nominal formation; (b) Formation translation; (c) Formation rotation; (d) Formation scaling; (e) Formation shearing along the X coordinate; and (f) Formation shearing along the Y coordinate.

The concept of affine formation manoeuvre control that applies the trick of stress matrices has recently emerged to address the challenges of formation manoeuvres for MASs. Unlike the conventional Laplacian matrix, the weight of each edge in a stress matrix can be any real number. This unique property provides a straightforward yet useful approach for formulating a distributed affine formation manoeuvre controller for MASs. Pioneering research on affine formation manoeuvres for single and double integrator MASs was done in [1]. Chen *et al.* expanded on this by exploring affine formation manoeuvre control for general linear MASs connected via undirected graphs [3]. In parallel, Xu *et al.* investigated the same problem but considered directed graphs and the issue of communication time delays [10]. More recently, in [11], historical velocity information was applied in designing a distributed controller for single integrator MASs, aiming to improve the efficiency of affine formation manoeuvres. However, previous research on affine formation manoeuvres for MASs either requires full-state feedback [1], [3], [10] or relies on velocity information [11], which may not be applicable in scenarios where such information is unavailable.

Lately, Negative Imaginary (NI) systems theory has shown promising applications in controlling MASs, including robotic arms [12], mobile vehicles [13], unmanned

This work was supported by the Engineering and Physical Sciences Research Council (EPSRC) [grant number EP/R008876/1] and the Science and Engineering Research Board (SERB), DST, India [grant numbers SRG/2022/000892 and CRG/2022/006114]. All research data supporting this publication are directly available within this publication. For the purpose of open access, the authors have applied a Creative Commons Attribution (CC BY) licence to any Author Accepted Manuscript version arising.

P. Bhowmick belongs to the Department of EEE, IIT Guwahati, Assam - 781039, India. A. Lanzon and Y.-H. Su belong to the Control Systems and Robotics Group, Department of EEE, University of Manchester, UK. Emails: Yu-Hsiang.Su@manchester.ac.uk, parijat.bhowmick@iitg.ac.in, Alexander.Lanzon@manchester.ac.uk.

aerial vehicles [14]–[16], and aircraft platoons [17]. The NI systems property, first introduced in [18], is commonly observed in flexible structures with collocated force actuators and position sensors [19], [20]. The idea of employing the NI systems theory in controlling MASs has stemmed from the fact that many MASs can be feedback-linearised or modelled as single or double integrator systems, which inherently exhibit NI properties. Therefore, a distributed Strictly Negative Imaginary (SNI) controller can be designed to stabilise such networked systems [14]. This work is motivated by the limitations associated with the full-state feedback requirement in previous research on affine formation manoeuvre control and builds on advancements made in applying the NI systems theory to control MASs. This paper develops a novel output-feedback-based control framework using the NI systems theory to achieve affine formation manoeuvres for MASs. Compared to existing approaches, the proposed control framework provides several advantages.

- It relies only on output feedback, specifically relative position measurements, making it suitable for scenarios where full-state measurements are unavailable. In addition, it minimises the sensor requirements;
- It provides more freedom in choosing a dynamic transfer function for formulating the distributed controller, thereby improving the formation tracking performance;

The set of real numbers is denoted by $\mathbb{R}$. The column vector with all N entries equal to 1 is denoted by $\mathbf{1}_N$. The 2-norm of a vector is denoted by $\|\cdot\|$. A positive definite (or semidefinite) matrix $A = A^\top$ is denoted by $A > 0$ (or ≥ 0). The complex conjugate transpose of a matrix A is denoted by A^*. The i^{th} eigenvalue of a matrix A is denoted by $\lambda_i[A]$. The rank of a matrix A is denoted by $\text{rank}(A)$. The Kronecker product of matrices A and B is represented by $A \otimes B$. $\mathcal{R}^{m\times n}$ denotes the space of all real, rational, proper transfer function matrices of dimension $(m \times n)$.

II. Technical Background and Problem Formulation

A. Graph, configuration, and formation

We use an undirected graph, denoted by $\mathcal{G} = \{\mathcal{V}, \mathcal{E}\}$, to describe the interaction topology among the networked agents, where $\mathcal{V} = \{1, 2, \cdots, N\}$ is the set of nodes, and $\mathcal{E} \subseteq \mathcal{V} \times \mathcal{V}$ is the set of all edges. The edge $e_{ij} = (i, j) \in \mathcal{E}$ indicates information exchange between the i^{th} and j^{th} nodes. For an undirected graph, the existence of $e_{ij} \in \mathcal{E}$ implies the existence of $e_{ji} \in \mathcal{E}$. The set $\mathcal{N}_i = \{j : (i, j) \in \mathcal{E}\}$ stands for the set of all neighbours of the i^{th} node.

A *configuration* is a pattern in the n-dimensional Euclidean plane $\mathbb{R}^n$, expressed by the coordinates of the nodes, denoted as $y_i \in \mathbb{R}^n \ \forall i \in \{1, 2, \ldots, N\}$. In this work, this configuration is represented by the cumulative position vector of the networked agents, represented as $\mathbf{y} \triangleq [y_1^\top, y_2^\top, \cdots, y_N^\top] \in \mathbb{R}^{nN}$. A *formation* in $\mathbb{R}^n$, denoted by $\mathcal{F} = (\mathcal{G}, \mathbf{y})$, is generated from a configuration $\mathbf{y}$ with an undirected graph $\mathcal{G}$ having N nodes and l edges.

B. Affine span and affine image

For a set of coordinates $\{y_i\}_{i=1}^N$ in $\mathbb{R}^n$, the associated *affine span* is defined as

$$\mathcal{S} = \left\{ \sum_{i=1}^{N} s_i y_i : s_i \in \mathbb{R} \ \forall i \text{ and } \sum_{i=1}^{N} s_i = 1 \right\}, \qquad (1)$$

where s_i is a scalar. If the dimension of $\mathcal{S}$ is equal to n, the set of coordinates $\{y_i\}_{i=1}^N$ is said to *affinely span* $\mathbb{R}^n$. This set is called *affinely independent* if there exists a set of scalars $\{s_i\}_{i=1}^N$, which contains at least one non-zero value, such that $\sum_{i=1}^N s_i y_i = 0$ and $\sum_{i=1}^N s_i = 0$; otherwise, it is called *affinely dependent*. If $\{y_i\}_{i=1}^N$ affinely span $\mathbb{R}^n$, there must be at least $(n+1)$ affinely independent coordinates [1].

A *nominal configuration* is defined by the cumulative vector $\mathbf{r} \triangleq [r_1^\top, r_2^\top, \cdots, r_N^\top]^\top \in \mathbb{R}^{nN}$. The *affine image* of this nominal configuration $\mathbf{r}$ is defined as

$$\mathcal{H}(\mathbf{r}) = \left\{ \mathbf{y} \in \mathbb{R}^{nN} : \mathbf{y} = (I_N \otimes A)\, \mathbf{r} + \mathbf{1}_N \otimes b \right\}, \qquad (2)$$

where $A \in \mathbb{R}^{n\times n}$ and $b \in \mathbb{R}^n$. The affine image contains all possible affine transformations of the nominal configuration $\mathbf{r}$, as shown in Fig. 1.

C. Stress matrix

Let a scalar $\omega_{ij} = \omega_{ji} \in \mathbb{R}$ be the weight of the edge e_{ij} in the formation $\mathcal{F}$. According to [1], [2], a stress matrix, denoted by $\Omega = [\Omega_{ij}] \in \mathbb{R}^{N\times N}$, is defined as follows:

$$\Omega_{ij} = \begin{cases} 0, & \text{if } i \neq j \text{ and } e_{ij} \notin \mathcal{E}, \\ -\omega_{ij}, & \text{if } i \neq j \text{ and } e_{ij} \in \mathcal{E}, \\ \sum_{k\in\mathcal{N}_i} \omega_{ik}, & \text{if } i = j. \end{cases} \qquad (3)$$

Definition 1: (**Equilibrium stress matrices**) [21]. For a given formation $\mathcal{F}$, its associated stress matrix Ω is called an equilibrium stress matrix if $(\Omega \otimes I_N)\, \mathbf{y} = 0$.

Remark 1: The structure of a stress matrix is similar to that of a Laplacian matrix. However, the weights of the edges forming a stress matrix can be any real number, unlike the constraints in a Laplacian matrix, which are limited to non-negative numbers.

Lemma 1: (**Universal rigidity**) [21]. A formation $\mathcal{F}$ is said to be universally rigid if and only if there exists a stress matrix $\Omega \geq 0$, satisfying $\text{rank}(\Omega) = N - n - 1$.

D. NI and SNI definitions

Definition 2: (**NI definition**) [18]. An LTI system with $D(s) \in \mathcal{R}^{m\times m}$ is called an NI system if: (a) there are no right-half plane poles; (b) $j[D(j\omega) - D(j\omega)^*] \geq 0 \ \forall \omega \in (0, \infty)$ except the values of ω where $s = j\omega$ is a pole of $D(s)$; (c) $s = j\omega_0$ with $\omega_0 \in (0, \infty)$ is a pole of $D(s)$, then it is at most a simple pole and $\lim_{s\to j\omega_0} (s - j\omega_0) j D(s) \geq 0$; and (d) $s = 0$ is a pole of $D(s)$, then $\lim_{s\to 0} s^k D(s) \geq 0 \ \forall k \geq 3$ and $\lim_{s\to 0} s^2 D(s) \geq 0$.

Definition 3: (**SNI definition**) [18]. An LTI system with $D(s) \in \mathcal{RH}_\infty^{m\times m}$ is called an SNI system if $j\,[D(j\omega) - D(j\omega)^*] > 0 \ \forall \omega \in (0, \infty)$.

E. Characteristic loci theory

The *characteristic loci* of a transfer function matrix $\Gamma(s)$, denoted as $\rho_i(s)\ \forall i \in \{1,2,\ldots,m\}$, characterise a conformal mapping of the complex function $\det[\Gamma(s)]$ onto a complex plane as s moves along the s-plane D-contour in a clockwise direction. Utilising the characteristic loci theory to establish the asymptotic stability of MIMO LTI systems can be linked to employing a multi-loop Nyquist criterion, providing a graphical stability tool for analysing MIMO system stability [22].

F. Problem statement

Consider a MAS consisting of N agents in $\mathbb{R}^n$, where $n \geq 2$ and $N > n+1$. These networked agents are connected by an undirected graph $\mathcal{G}$, with n_l leader agents and n_f follower agents. Let $\mathcal{V}_l = \{1,\ldots,n_l\}$ and $\mathcal{V}_f = \{n_{l+1},\ldots,N\}$ be the sets of leader agents and follower agents, respectively. The cumulative vectors $\mathbf{y}_l = [y_1^\top,\cdots,y_{n_l}^\top]^\top \in \mathbb{R}^{nn_l}$ and $\mathbf{y}_f = [y_{n_{l+1}}^\top,\cdots,y_N^\top]^\top \in \mathbb{R}^{nn_f}$ denote respectively the positions of all leader agents and follower agents. The dynamics of each follower agent are represented by a double integrator system: $\dot{y}_i = v_i,\ \dot{v}_i = u_i,\ \forall i \in \mathcal{V}_f$, where y_i is the position, v_i is the velocity, and u_i is the control input to be designed. Let $\bar{\Omega} = \Omega \otimes I_d$ be the associated stress matrix, which can be partitioned as $\bar{\Omega} = \left[\begin{array}{c|c} \bar{\Omega}_{ll} & \bar{\Omega}_{lf} \\ \hline \bar{\Omega}_{fl} & \bar{\Omega}_{ff} \end{array}\right]$, where $\bar{\Omega}_{ll} \in \mathbb{R}^{nn_l \times nn_l}$, $\bar{\Omega}_{lf} \in \mathbb{R}^{nn_l \times nn_f}$, $\bar{\Omega}_{fl} \in \mathbb{R}^{nn_f \times nn_l}$ and $\bar{\Omega}_{ff} \in \mathbb{R}^{nn_f \times nn_f}$.

The primary control objective is to develop a dynamic output-feedback cooperative control framework for follower agents to achieve affine formation manoeuvres, relying only on relative position measurements of the agents. The proposed framework aims to drive the follower agents to reach their desired positions $\mathbf{y}_f^*(t)$ within the target formation $\mathcal{F}$, that is

$$\lim_{t\to\infty} \big(\mathbf{y}_f(t) - \mathbf{y}_f^*(t)\big) = 0. \tag{4}$$

We will now introduce a crucial condition guaranteeing that the desired positions of the leader agents, denoted as $\mathbf{y}_l^*(t)$, uniquely determine (in fact, dictate) the desired positions of the follower agents, denoted as $\mathbf{y}_f^*(t)$.

Lemma 2: (**Affine localisability**) [1]. Given a nominal formation $\mathcal{F}_r = (\mathcal{G},\mathbf{r})$ and a configuration $\mathbf{y} = [\mathbf{y}_l^\top,\mathbf{y}_f^\top]^\top \in \mathcal{H}(\mathbf{r})$, $\mathbf{y}_l$ can uniquely determine $\mathbf{y}_f$ if and only if $\{r_i\}_{i\in\mathcal{V}_l}$ affinely span $\mathbb{R}^n$.

Assumption 1: We assume that the nominal formation $\mathcal{F}_r$ is universally rigid and $\{r_i\}_{i\in\mathcal{V}_l}$ affinely span $\mathbb{R}^n$.

According to [1], the following relationship between the desired positions of leaders and followers can be readily established:

$$\mathbf{y}_f^*(t) = -\bar{\Omega}_{ff}^{-1}\bar{\Omega}_{fl}\mathbf{y}_l^*(t) \tag{5}$$

via the property $\bar{\Omega}_{ff} > 0$ implied by Lemma 2.

III. Formation manoeuvres design

Consider a nominal formation $\mathcal{F}_r$, which represents a static formation as shown in Fig. 1(a). The desired configuration $\mathbf{y}^*(t)$ within the target formation $\mathcal{F}$ can be described as follows:

$$\mathbf{y}^*(t) = (I_N \otimes A(t))\,\mathbf{r} + \mathbf{1}_N \otimes b(t), \tag{6}$$

where $A(t) \in \mathbb{R}^{n\times n}$ and $b(t) \in \mathbb{R}^n$ are defined as the affine transformation matrices designed to achieve formation manoeuvring actions. The desired position $y_i^*(t)$ of each agent i can then be expressed as:

$$y_i^*(t) = A(t)r_i + b(t) \quad \forall i \in \mathcal{V}. \tag{7}$$

We will now design the affine transformation matrices $A(t)$ and $b(t)$ to achieve formation manoeuvres in $\mathbb{R}^2$, including translation, rotation, scaling and shearing.

A. Formation translation design

To achieve formation translational motion, we design

$$b(t) = \begin{bmatrix} b_x(t) \\ b_y(t) \end{bmatrix},\ \dot{b}_x(t) = \dot{b}_x^*,\ \dot{b}_y(t) = \dot{b}_y^*, \tag{8}$$

where $b_x(t)$ and $b_y(t)$ are the translational movements w.r.t. the nominal formation $\mathcal{F}_r$ in the X and Y coordinates, as shown in Fig. 1(b), and $\dot{b}_x^*$ and $\dot{b}_y^*$ are the desired velocities in each coordinate, as specified by the users.

B. Formation rotation design

To achieve formation rotational motion, we design

$$A(t) = R(\theta(t)) = \begin{bmatrix} \cos\theta(t) & -\sin\theta(t) \\ \sin\theta(t) & \cos\theta(t) \end{bmatrix},\ \dot{\theta}(t) = \dot{\theta}^*, \tag{9}$$

where $\theta(t)$ denotes the rotation angle w.r.t. the nominal formation $\mathcal{F}_r$, as depicted in Fig. 1(c), and $\dot{\theta}^*$ is the desired rotation rate, as specified by the users.

C. Formation scaling design

To achieve formation scaling motion, we design

$$A(t) = \begin{bmatrix} s_x(t) & 0 \\ 0 & s_y(t) \end{bmatrix},\ \dot{s}_x(t) = \dot{s}_x^*,\ \dot{s}_y(t) = \dot{s}_y^*, \tag{10}$$

where $s_x(t)$ and $s_y(t)$ are the scaling factors w.r.t. the nominal formation $\mathcal{F}_r$ in the X and Y coordinates, as shown in Fig. 1(d), and $\dot{s}_x^*$ and $\dot{s}_y^*$ are the desired scaling rates in each coordinate, as specified by the users.

D. Formation shearing design

To achieve formation shearing motion in the X coordinate, we design

$$A(t) = \begin{bmatrix} 1 & \tan\phi(t) \\ 0 & \psi_y(t) \end{bmatrix},\ \dot{\phi}(t) = \dot{\phi}^*, \tag{11}$$

where $\psi_y(t) \in \{0,1\}$, $\phi(t)$ denotes the shearing angle w.r.t. the nominal formation $\mathcal{F}_r$, as depicted in Fig. 1(e), and $\dot{\phi}^*$ is the desired shearing rate, as specified by the users. When $\psi_y(t) = 0$, the target formation $\mathcal{F}$ is collinear in the X coordinate. Similarly, to achieve formation shearing motion in the Y coordinate, we design

$$A(t) = \begin{bmatrix} \psi_x(t) & 0 \\ \tan\phi(t) & 1 \end{bmatrix},\ \dot{\phi}(t) = \dot{\phi}^*, \tag{12}$$

where $\psi_x(t) \in \{0,1\}$, $\phi(t)$ denotes the shearing angle w.r.t. the nominal formation $\mathcal{F}_r$, as depicted in Fig. 1(f), and $\dot{\phi}^*$ is the desired shearing rate. When $\psi_x(t) = 0$, the target formation $\mathcal{F}$ is collinear in the Y coordinate.

IV. Output affine formation manoeuvre control

A. Distributed SNI systems properties

The following two Lemmas establish the properties of networked SNI systems with a nominal formation $\mathcal{F}_r$ that satisfies Assumption 1.

Lemma 3: Consider a distributed SNI system represented by $\hat{\Sigma}_c(s) \triangleq \bar{\Omega}_{ff} \otimes \Sigma_c(s)$ with a nominal formation $\mathcal{F}_r$ satisfying Assumption 1. Then, $\hat{\Sigma}_c(s)$ is SNI if and only if $\Sigma_c(s)$ is SNI.

Proof. (Sufficiency) Given that $\Sigma_c(s)$ is SNI, it satisfies $j[\Sigma_c(j\omega) - \Sigma_c(j\omega)^*] > 0 \ \forall \omega \in (0, \infty)$. Assumption 1 ensures $\bar{\Omega}_{ff} = \bar{\Omega}_{ff}^\top > 0$. Now, utilising the Kronecker product property $A \otimes B > 0$ when $A = A^* > 0$ and $B = B^* > 0$ [23], we have $j[\hat{\Sigma}_c(j\omega) - \hat{\Sigma}_c(j\omega)^*] = j[\bar{\Omega}_{ff} \otimes \Sigma_c(j\omega) - \bar{\Omega}_{ff}^\top \otimes \Sigma_c(j\omega)^*] = \bar{\Omega}_{ff} \otimes j[\Sigma_c(j\omega) - \Sigma_c(j\omega)^*] > 0 \ \forall \omega \in (0, \infty)$. Therefore, $\hat{\Sigma}_c(s)$ is SNI.

(Necessity). Staring with the condition that $\hat{\Sigma}_c(s)$ is SNI, that is, $j[\hat{\Sigma}_c(j\omega) - \hat{\Sigma}_c(j\omega)^*] > 0 \ \forall \omega \in (0, \infty)$, it implies $j[\Sigma_c(j\omega) - \Sigma_c(j\omega)^*] > 0 \ \forall \omega \in (0, \infty)$ since $\bar{\Omega}_{ff} = \bar{\Omega}_{ff}^\top > 0$ via Assumption 1. This completes the proof. ■

Lemma 4: Consider a distributed SNI system represented by $\hat{\Sigma}_c(s) \triangleq \bar{\Omega}_{ff} \otimes \Sigma_c(s)$ with a nominal formation $\mathcal{F}_r$ satisfying Assumption 1. Then, $\hat{\Sigma}_c(0) < 0$ (or > 0) if and only if $\Sigma_c(0) < 0$ (or > 0).

Proof. (Sufficiency) We start with noting that $\bar{\Omega}_{ff} > 0$ via Assumption 1. Utilising the property $\lambda_k[A \otimes B] = \lambda_i[A]\lambda_j[B]$ where $A \in \mathbb{R}^{m \times m}$, $B \in \mathbb{R}^{n \times n}$ and $k \in \{1, 2, \ldots, mn\}$ (including the multiplicities) [23], we have $\hat{\Sigma}_c(0) = \bar{\Omega}_{ff} \otimes \Sigma_c(0) < 0$ (or > 0) when $\Sigma_c(0) < 0$ (or > 0).

(Necessity) The condition $\hat{\Sigma}_c(0) = \bar{\Omega}_{ff} \otimes \Sigma_c(0) < 0$ (or > 0) readily implies $\Sigma_c(0) < 0$ (or > 0), as $\bar{\Omega}_{ff} > 0$ via Assumption 1. This completes the proof. ■

B. Output-feedback affine formation manoeuvre control applying NI toolkit

Recall that the control objective for achieving output affine formation manoeuvres is to steer the follower agents to their desired positions $\mathbf{y}_f^*(t)$ within the target formation $\mathcal{F}$ using only output feedback, i.e., relative position measurements. Now, the formation tracking error for the follower agent, denoted as $e_i(t)$, is defined as follows:

$$e_i(t) = y_i(t) - y_i^*(t) \quad \forall i \in \mathcal{V}_f. \tag{13}$$

Then, the formation tracking error for all follower agents, denoted as $\mathbf{e}(t)$, can be expressed as follows:

$$\mathbf{e}(t) = \mathbf{y}_f(t) - \mathbf{y}_f^*(t) = \mathbf{y}_f(t) + \bar{\Omega}_{ff}^{-1}\bar{\Omega}_{fl}\mathbf{y}_l^*(t). \tag{14}$$

We are now prepared to introduce the main theorem, which presents an SNI-based output-feedback affine formation manoeuvre control framework, as shown in Fig. 2, employing the NI systems theory. In the upcoming theorem, the notations $U_i(s)$ and $Y_i(s)$ denote the Laplace Transform of the real-valued time-domain signals $u_i(t)$ and $y_i(t)$, respectively, for all $t \geq 0$ and all i.

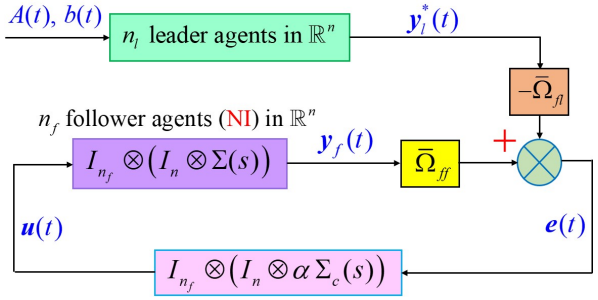

Fig. 2. An SNI-based output-feedback affine formation manoeuvre control framework, where $\Sigma(s)$ represents a double-integrator NI follower agent and $\Sigma_c(s)$ is an SNI controller.

Theorem 1: Consider a homogeneous MAS with n_l leader agents and n_f followers agents whose dynamics can be represented by a networked double integrator system. Assume that the interaction topology $\mathcal{G}$ and the nominal formation $\mathcal{F}_r = (\mathcal{G}, \mathbf{r})$ satisfy Assumption 1. Let $\Sigma_c(s)$ be an SNI controller with $\Sigma_c(0) < 0$, and $\alpha \in (0, \infty)$ be a parameter. Then, through the following output-feedback distributed SNI control law:

$$U_i(s) = \alpha\Sigma_c(s) \sum_{j \in \mathcal{N}_i} \omega_{ij} \left(Y_i(s) - Y_j(s)\right) \quad \forall i \in \mathcal{V}_f, \tag{15}$$

the follower agents achieve affine formation manoeuvres and track their desired positions within the target formation.

Proof. We will first show the asymptotic stability of the affine formation manoeuvre control framework, as depicted in Fig. 2, by exploiting the characteristic loci theorem [22]. The proof builds on the arguments presented in [14, Theorem 2]. The loop transfer function matrix in Fig. 2 can be expressed as $L(s) = \bar{\Omega}_{ff} \otimes (\Sigma_c(s)\Sigma(s))$, where $\Sigma(s) = \frac{1}{s^2}$ is the model of each follower, $\Sigma_c(s)$ is an SNI controller selected such that $\Sigma_c(0) < 0$ and $\bar{\Omega}_{ff} > 0$. Following the proof of [14, Theorem 2], it can be established that none of the characteristic loci of $L(s)$ encircle the critical point $(\frac{1}{\alpha} + j0)$ for any $\alpha \in (0, \infty)$. This confirms the asymptotic stability of the overall closed-loop networked system.

Next, we will show the asymptotic convergence of the formation tracking error $\mathbf{e}(t)$. From Fig. 2, we can readily obtain the transfer function representation of the error dynamics as $\mathbf{E}(s) = \left[I - \left(\bar{\Omega}_{ff} \otimes (\alpha\Sigma_c(s)\Sigma(s))\right)\right]^{-1}$. Then, the expression for the steady-state error in the time domain can be obtained as follows:

$$\begin{aligned}
\mathbf{e}_{ss} &= \lim_{t \to \infty} \mathbf{e}(t) = \lim_{s \to 0} s\, \mathbf{E}(s) \\
&= \lim_{s \to 0} s \left[I - \left(\bar{\Omega}_{ff} \otimes (\alpha\Sigma_c(s)\Sigma(s))\right)\right]^{-1} \left(\bar{\Omega}_{fl}\mathbf{Y}_l(s)\right) \\
&= \lim_{s \to 0} s^2 \left[s^2 I - \left(\bar{\Omega}_{ff} \otimes (\alpha\Sigma_c(s))\right)\right]^{-1} \left(s\bar{\Omega}_{fl}\mathbf{Y}_l(s)\right) \\
&= -\left[\alpha\hat{\Sigma}_c(0)\right]^{-1} \left(\lim_{s \to 0} s^2 I\right) \times \left(\lim_{s \to 0} s\bar{\Omega}_{fl}\mathbf{Y}_l(s)\right).
\end{aligned}$$

Since $\hat{\Sigma}_c(0) < 0$ via Lemma 4, $\bar{\Omega}_{fl}$ is a bounded real matrix, and $\mathbf{y}_l(t)$ is an $\mathcal{L}_\infty$-bounded signal admitting a steady-state, the above expression reduces to $\mathbf{e}_{ss} = [0, 0, \ldots, 0]^\top$. This implies that $\lim_{t \to \infty} \left(\mathbf{y}_f(t) - \mathbf{y}_f^*(t)\right) = 0$, i.e., the condition

given in (4) holds. Therefore, we conclude that all follower agents track their desired positions within the target formation. This completes the proof. ■

Remark 2: Note that the affine transformation matrices $A(t)$ and $b(t)$ are only shared among leader agents. Follower agents do not directly access this information; however, they achieve affine formation manoeuvres and track their desired positions within the target formation by tracking the motions of those leader agents via the proposed output-feedback distributed SNI control law in (15).

C. An extension to heterogeneous NI MASs

To this end, we propose an extension of the SNI-based affine formation manoeuvre control framework to *heterogeneous* NI agents, as depicted in Fig. 3. Assume that the interaction topology $\mathcal{G}$ and the nominal formation $\mathcal{F}_r$ satisfy Assumption 1. Let Ω_{ff} be decomposed as $Q_{ff}\mathbb{W}Q_{ff}^\top$, where $Q_{ff} \in \mathbb{R}^{n_f \times l}$ is an incidence matrix associated with Ω_{ff}, and $\mathbb{W} = \operatorname{diag}\{w_k\} \in \mathbb{R}^{l\times l}$ is the weight matrix containing the weights of the edges connecting the followers among themselves and with the leaders. Choose a set of stable controllers $\Sigma_{c,k}(s)$ for $k \in \{1, 2, \ldots, l\}$ such that $\operatorname{diag}_{k=1}^{l}\{w_k\Sigma_{c,k}(s)\}$ is SNI with $w_k\Sigma_{c,k}(0) < 0$. Then, through the following output-feedback distributed SNI control law

$$U_i(s) = \alpha_i \sum_{j\in\mathcal{N}_i} \omega_{ij}\, \Sigma_{c,k}(s)\big(Y_i(s) - Y_j(s)\big) \quad \forall i \in \mathcal{V}_f, \quad (16)$$

the heterogeneous NI agents achieve affine formation manoeuvres and track their desired positions.

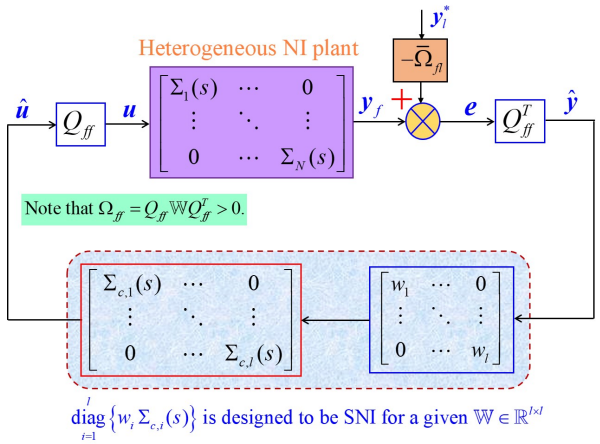

Fig. 3. An affine formation manoeuvre control framework for heterogeneous NI MASs with a split-arrangement of its stress matrix $\Omega_{ff} = Q_{ff}\mathbb{W}Q_{ff}^\top$.

V. Simulation Case Study

We conducted a MATLAB simulation case study involving a team of seven networked agents operating in a two-dimensional space to demonstrate the feasibility of the proposed SNI-based output-feedback affine formation manoeuvre control framework. Fig. 4 describes the interaction topology among these networked agents, with the weight ω_{ij} assigned to each edge. The affine transformation matrices

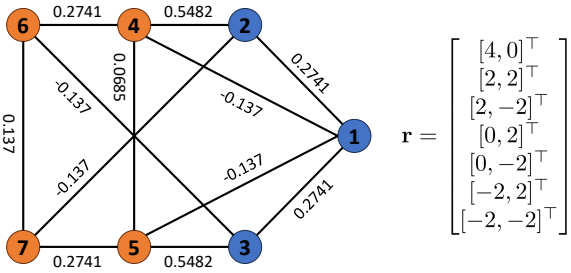

Fig. 4. The interaction topology, the weight of each edge, and the nominal configuration for the MATLAB simulation case study. Agents $1-3$ are the leader agents, and agents $4-7$ are the follower agents

$A(t)$ and $b(t)$ were designed in advance using Equations (8)–(12), ensuring that all networked agents could safely navigate through a cluttered environment. The objective was for the follower agents to achieve affine formation manoeuvres and track their desired positions by implementing the proposed control law in (15). In this simulation, we selected an SNI controller transfer function $\Sigma_c(s) = -\left(\frac{s+1}{s+10}\right)$ with $\Sigma_c(0) < 0$ and $\alpha = 200$ to be implemented in (15).

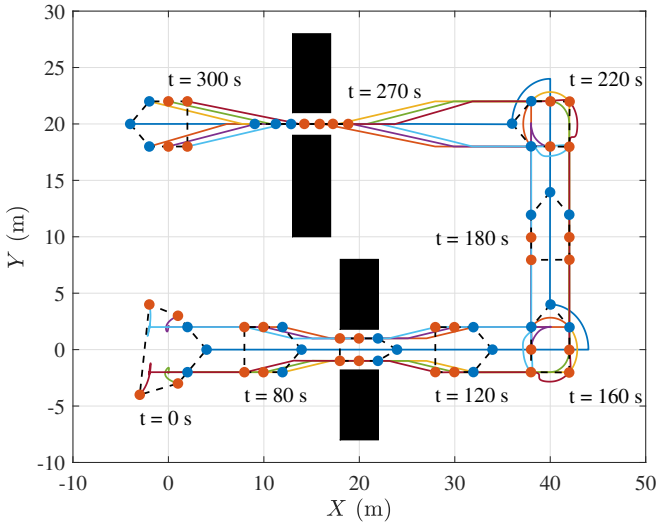

Fig. 5. The trajectories of all networked agents in a two-dimensional space. Leader agents are denoted by blue circles, follower agents by orange circles, and obstacles by black rectangles. Black dashed lines mark the formation at each time stamp. A team of networked agents executed formation translation, rotation, scaling, and shearing by implementing the proposed SNI-based output-feedback affine formation manoeuvre control framework.

Fig. 5 shows the trajectories of networked agents in a two-dimensional space, demonstrating how leader agents dynamically adjusted the target formation through affine transformations to enable different formation manoeuvres. This adjustment ensures safe navigation through a cluttered environment with obstacles. With the proposed SNI control law in (15), all follower agents reached their desired positions within the target formation using only relative position measurements. Fig. 6(a) presents the 2-norm of the formation tracking error, showing rapid convergence to zero. Fig. 6(b) and Fig. 6(c) show the velocities of the followers. These results indicate that the networked agents have achieved the

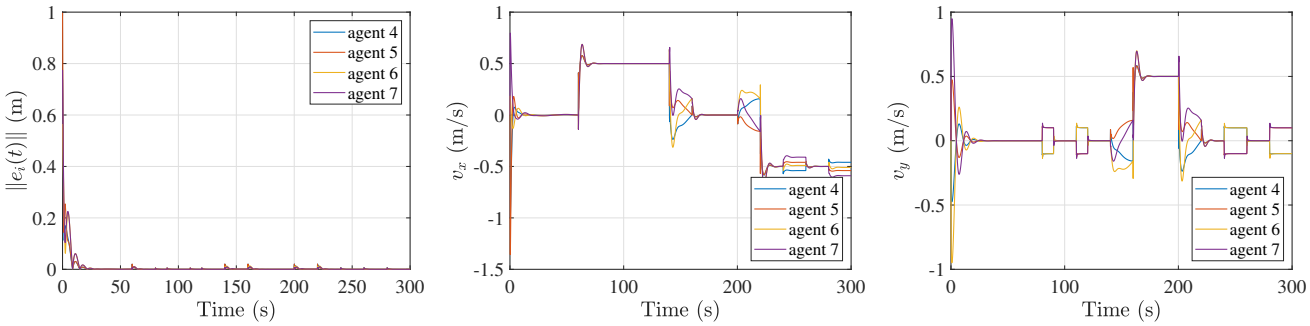

(a) Formation tracking error. (b) Velocity along the X coordinate. (c) Velocity along the Y coordinate.

Fig. 6. The 2-norms of the formation tracking errors and velocities for the follower agents.

desired affine formation manoeuvres via the proposed SNI-based output-feedback affine formation control framework.

VI. Conclusions

This paper addresses the output affine formation manoeuvre control problem for MASs by applying the NI systems theory. The proposed control framework relies only on output feedback, offering advantages such as reduced sensor requirements and an ideal solution in scenarios where full-state measurements are unavailable. The methodology begins with formulating affine transformation matrices for all leader agents, which dynamically adjusting from the nominal formation to the target formation. Following this, the proposed output-feedback distributed SNI control law enables follower agents to achieve affine formation manoeuvres. A comprehensive simulation case study demonstrates the feasibility and performance of the proposed control framework. Future work will include a rigorous analysis of extending this approach to heterogeneous NI MASs and its implementation in physical multi-robot systems.

References

[1] S. Zhao, "Affine Formation Maneuver Control of Multiagent Systems," *IEEE Transactions on Automatic Control*, vol. 63, no. 12, pp. 4140–4155, Dec. 2018.

[2] Z. Lin, L. Wang, Z. Chen, M. Fu, and Z. Han, "Necessary and Sufficient Graphical Conditions for Affine Formation Control," *IEEE Transactions on Automatic Control*, vol. 61, no. 10, pp. 2877–2891, Oct. 2016.

[3] L. Chen, J. Mei, C. Li, and G. Ma, "Distributed Leader–Follower Affine Formation Maneuver Control for High-Order Multiagent Systems," *IEEE Transactions on Automatic Control*, vol. 65, no. 11, pp. 4941–4948, Nov. 2020.

[4] Y.-H. Su and A. Lanzon, "Formation-containment tracking and scaling for multiple quadcopters with an application to choke-point navigation," in *Proceedings of the International Conference on Robotics and Automation*, May 2022, pp. 4908–4914.

[5] Y.-H. Su, P. Bhowmick, and A. Lanzon, "A Fixed-Time Formation-Containment Control Scheme for Multi-Agent Systems With Motion Planning: Applications to Quadcopter UAVs," *IEEE Transactions on Vehicular Technology*, vol. 73, no. 7, pp. 9495–9507, July 2024.

[6] ——, "A robust adaptive formation control methodology for networked multi-UAV systems with applications to cooperative payload transportation," *Control Engineering Practice*, vol. 138, p. 105608, Sept. 2023.

[7] H. Garcia de Marina, B. Jayawardhana, and M. Cao, "Distributed rotational and translational maneuvering of rigid formations and their applications," *IEEE Transactions on Robotics*, vol. 32, no. 3, pp. 684–697, June 2016.

[8] K. Wu, J. Hu, B. Lennox, and F. Arvin, "Finite-time bearing-only formation tracking of heterogeneous mobile robots with collision avoidance," *IEEE Transactions on Circuits and Systems II: Express Briefs*, vol. 68, no. 10, pp. 3316–3320, Oct. 2021.

[9] B. Wang, "A time-varying observer design for synchronization with an uncertain target and its applications in coordinated mission rendezvous," *Automatica*, vol. 136, p. 109931, Feb. 2022.

[10] Y. Xu, S. Zhao, D. Luo, and Y. You, "Affine formation maneuver control of high-order multi-agent systems over directed networks," *Automatica*, vol. 118, p. 109004, Aug. 2020.

[11] W. Yu, B. Zhu, X. Wang, P. Yi, H. Liu, and T. Hu, "Enhanced Affine Formation Maneuver Control Using Historical Velocity Command (HVC)," *IEEE Robotics and Automation Letters*, vol. 8, no. 11, pp. 7186–7193, Nov. 2023.

[12] O. Skeik and A. Lanzon, "Robust output consensus of homogeneous multi-agent systems with negative imaginary dynamics," *Automatica*, vol. 113, p. 108799, Mar. 2020.

[13] O. Skeik, J. Hu, F. Arvin, and A. Lanzon, "Cooperative control of integrator negative imaginary systems with application to rendezvous multiple mobile robots," in *Proceedings of the 12th International Workshop on Robot Motion and Control*, July 2019, pp. 15–20.

[14] Y.-H. Su, P. Bhowmick, and A. Lanzon, "A Negative Imaginary Theory-Based Time-Varying Group Formation Tracking Scheme for Multi-Robot Systems: Applications to Quadcopters," in *Proceedings of the IEEE International Conference on Robotics and Automation*, May 2023, pp. 1435–1441.

[15] ——, "Cooperative Control of Multi-Agent Negative Imaginary Systems with Applications to UAVs, Including Hardware Implementation Results," in *Proceedings of the European Control Conference*, June 2023.

[16] ——, "Properties of interconnected negative imaginary systems and extension to formation-containment control of networked multi-UAV systems with experimental validation results," *Asian Journal of Control*, Dec. 2023.

[17] ——, "A Negative Imaginary Solution to an Aircraft Platooning Problem," in *Proceedings of the European Control Conference*, June 2024, pp. 2580–2585.

[18] A. Lanzon and I. R. Petersen, "Stability robustness of a feedback interconnection of systems with negative imaginary frequency response," *IEEE Transactions on Automatic Control*, vol. 53, no. 4, pp. 1042–1046, May 2008.

[19] B. Bhikkaji, S. O. Reza Moheimani, and I. R. Petersen, "A negative imaginary approach to modeling and control of a collocated structure," *IEEE/ASME Transactions on Mechatronics*, vol. 17, no. 4, pp. 717–727, Aug. 2012.

[20] J. Wang, A. Lanzon, and I. R. Petersen, "Robust output feedback consensus for networked negative-imaginary systems," *IEEE Transactions on Automatic Control*, vol. 60, no. 9, pp. 2547–2552, Sept. 2015.

[21] R. Connelly, "Generic Global Rigidity," *Discrete & Computational Geometry*, vol. 33, no. 4, pp. 549–563, Apr. 2005.

[22] A. G. J. Macfarlane and J. J. Belletrutti, "The characteristic locus design method," *Automatica*, vol. 9, no. 5, pp. 575–588, 1973.

[23] R. A. Horn and C. R. Johnson, *Matrix Analysis*, 2nd ed. London, UK.: Cambridge University Press, 2013.